# Synergistic Fusion of GPS and Photogrammetrically Generated Elevation Models

**Jon P. Mills, Simon J. Buckley, and Harvey L. Mitchell**

## Abstract

*Digital elevation models (DEMs) produced from photogrammetric data sources have long relied on the use of ground control points to give them scale and orientation. However, in areas such as coastlines, landslides, or glaciers, where identification of suitable natural features and pre-marking is difficult, the use of conventional ground control may be unfeasible. This paper reports on research that uses independently collected DEMs derived from kinematic GPS to orient surfaces produced by aerial photogrammetric methods, using a least-squares surface matching algorithm. During algorithm development, three stages of testing were carried out, using increasingly more complex datasets. Initially, simulated surfaces were used to validate the matching theory and program. Then, a DEM derived from conventional aerial photography was matched with a GPS model, highlighting the effectiveness of surface matching to recover systematic errors in datasets. Finally, surfaces derived from small format digital imagery were successfully fused with wireframe GPS surfaces, the high redundancy and automation potential creating an elegant and cheaper alternative to photocontrol.*

## Introduction

Traditionally, photogrammetric processing has relied on a set of independently measured ground control points (GCPs) to scale and orientate stereomodels by relating them to an object-space reference coordinate system (e.g., Wolf and Dewitt, 2000). For monitoring purposes, it is often necessary to create high-resolution DEMs at different epochs, but in the same coordinate system, in order to allow accurate change detection (Cooper, 1998). Often, monitored areas are least suited to natural GCP identification, due to the dynamic processes that require measurement, such as landslides (Brunsden and Chandler, 1996), glacial movement (Baltsavias *et al.*, 2001), and coastal erosion (Adams and Chandler, 2002). This absolute orientation stage has long been the most inefficient part of the photogrammetric flowline, as well as having the least potential for automation (Schenk, 1999).

Modern automated aerial triangulation methods employed in digital photogrammetry have meant that the amount of required photocontrol, formerly a minimum of three height and two plan points per stereopair (Rosenholm and Torlegård, 1988), has been greatly reduced. However, in areas such as coastlines or landslides where few "hard" natural or manmade features exist, the identification and acquisition of ground control is made more difficult and time consuming (Warner *et al.*, 1996). A common solution to this problem is the use of prefabricated control markers, positioned and coordinated before a photographic mission, but increased expense and unpredictable weather conditions still make for inadequacy (Baltsavias *et al.*, 2001). The use of kinematic Global Positioning System (GPS) equipment and inertial systems to determine the exposure station coordinates has further reduced the need for photocontrol (Wolf and Dewitt, 2000), but increased expense and complication, as well as calibration difficulties (Cramer *et al.*, 2000) make it inappropriate for low-cost surveys.

A potential alternative solution is to use an existing DEM to orientate a photogrammetric elevation model produced after only the relative stage of orientation, in effect using a control surface to provide absolute orientation, rather than using discrete points (Schenk, 1999). The use of a terrain surface means that the DEM can be collected independently of the photography, and is not reliant on the presence and identification of visible ground features. The problem is instead to register the unorientated photogrammetric elevation model to the absolute coordinate system of the existing ground DEM. Research has been carried out previously in the area of surface matching, with methods ranging in complexity. Ebner and Strunz (1988) and Rosenholm and Torlegaård (1988) developed the absolute orientation of large blocks of aerial imagery using coarse national-level DEMs, by minimizing the vertical differences between surfaces in a least-squares based adjustment. Pilgrim (1991), Karras and Petsa (1993), and most recently Mitchell and Chadwick (1999) used surface matching to detect deformations between sets of ultra-small-scale surfaces at different intervals for medical applications, where the use of control markers is undesirable and unethical. Schenk (1999) and Habib *et al.* (2001) used a variation of this surface matching technique, by minimizing the distances between normals of the two surfaces, with reference to absolute orientation of imagery and change detection.

Further application areas of surface matching have been seen in comparisons between photogrammetric and lidar derived surfaces (Habib *et al.*, 2000), as well as recovering shifts between strips of lidar data (Maas, 2000). The Iterative Closest Point (ICP) algorithm (Besl and Mckay, 1992) has been developed in the field of computer vision to fully match three-dimensional surfaces. However, as noted by Mitchell and Chadwick (1999), its relative complexity may be unnecessary for conventional 2½ D topographic surfaces. Consequently, least-squares minimization of vertical differences forms the basis of this research, part of an ongoing project developing an optimum solution for monitoring coastal erosion, by removing

J.P. Mills and S.J. Buckley are with the School of Civil Engineering and Geosciences, University of Newcastle upon Tyne, Tyne and Wear NE1 7RU, United Kingdom (j.p.mills@ncl.ac.uk).

H.L. Mitchell is with the School of Engineering, University of Newcastle, Newcastle, New South Wales 2308, Australia.

Photogrammetric Engineering & Remote Sensing
Vol. 69, No. 4, April 2003, pp. 341–349.

0099-1112/03/6904–341$3.00/0

the need for photocontrol to orientate large strips of small-format digital imagery. Use of a small-format digital camera results in a large number of images covering the coastal zone; however, the use is justified by the narrow area of interest of the coastal strip, combined with the practicalities of instantly available digital imagery. Even with sophisticated aerial triangulation techniques available in modern digital photogrammetric workstations, a correspondingly large amount of photocontrol points would be required. Because of the dynamic nature of the coastal zone (Adams and Chandler, 2002), it is ill suited for the collection of naturally occurring or built features; thus, prefabricated markers would need to be used. The main problem with this approach is its tide and weather dependency, meaning that markers would have to be laid over the coastal zone and coordinated in a short time window, ready for a flight to take place (Warner *et al.*, 1996).

## Problem Specification

Although some relevant peculiarities of the surface matching algorithm are discussed below, it is not within the scope of this paper to fully derive the least-squares surface matching theory. Mitchell and Chadwick (1999), Rosenholm and Torlegård (1988), and Karras and Petsa (1993) instead provide all details of the derivation. The primary function of this paper is to report on developments of the fundamental matching algorithm and findings related to its application for photogrammetric control, a case in which the surfaces have an irregular and sometimes complex point distribution. The problem is to assess the viability and accuracy of the matching process for these purposes when used in practice.

During photogrammetric processing, imagery is taken to the relative orientation stage so that an elevation model can be generated but it exists in an arbitrary coordinate system, independent of any reference system. The problem then is to relate this floating elevation model to an existing DEM of limited extent. This corresponds to finding the necessary transformation parameters allowing the photogrammetric surface to be rotated, translated, and scaled into the existing DEM coordinate system. The procedure is complicated by a number of conditions (Schenk, 1999) caused by the use of dissimilar datasets, both in terms of configuration, data collection, and actual surface differences, meaning that no conjugate control points may be identifiable between the models to carry out the transformation.

Based on these assumptions, a match is needed to relate the two surfaces, that may have differences, with the best possible fit. The solution is based on the 3D conformal transformation, a standard seven-parameter adjustment relating two sets of known points in separate coordinate systems using three translations ($T_x$, $T_y$, $T_z$), three rotations ($\omega$, $\phi$, $\kappa$), and a scale parameter ($s$) (Wolf and Dewitt, 2000). As noted above, control points may not exist to relate the two surfaces to be matched, so a different approach is used in surface matching, where each point in one DEM can be considered to provide control information, and the best fit is found by minimizing the surface differences.

## Surface Matching Algorithm

The surface matching consists of solution for the seven transformation parameters given above, by minimizing the sum of the squares of vertical differences ($\delta Z$) between the surfaces at points $i$: i.e.,

$$\delta Z_i = a_{i1}\Delta T_x + a_{i2}\Delta T_y + a_{i3}\Delta T_z a_{i4}\Delta\omega + a_{i5}\Delta\phi + a_{i6}\Delta\kappa + a_{i7}\Delta s \quad (1)$$

where $\Delta$ prefixes signify corrections to initial values of parameters, and the $a_{ij}$ represent the coefficient of the $j$th parameter.

Various numerical and practical problems arise in the implementation of this calculation. First, the solution relies on finding conjugate points on the second surface, so that the two surfaces are brought into alignment. For regular gridded data, with the same surface shape and integer shift values, this is relatively simple to solve. However, if the data are irregular, or are collected using two different measurement techniques, the surfaces may be sampled at points which are distributed differently. Indeed this scenario may be complicated by the fact that *no* points may be in common, so that the two surfaces to be matched are only similar. If the data describing the two surfaces have been collected using different methods, in effect it is as though there has been 100 percent surface deformation. The implications of this on the matching algorithm are that there will always be some errors, or parameter deviations, introduced due to the differences in surface description.

The crux of the surface matching problem relies on finding conjugate points between the surfaces; in the traditional photogrammetric route, this information is already known, because the only data that exist are the control points. For surface matching, each point is treated as a control point in height, with exclusions based on outliers. However, if the two surfaces are in different reference systems, as is assumed, and ungridded data of different surface areas are used, finding conjugate points is more difficult. Suppose that two surfaces are to be matched, surface one and surface two. Instead of simply taking the nearest point on surface two to a point on surface one and using its height value, a better approximation can be made with the enclosing surface patch. Using the Delaunay triangulation (McCullagh, 1990) of surface one gives a table of triangles describing the surface, rather than a disjointed set of points. This can be used to find the enclosing triangle in the triangulation for a point on surface two, enabling a better $Z$-value to be interpolated than if a single closest point was used. Clearly, any consistently large differences between the interpolated height values will imply that the surfaces are not in the correct position and transformation will take place during solving of the least-squares solution.

Second, because of the discrete nature of the surface, which is attempting to represent a continuous function, gradient values can only be approximated using surrounding points. If the surface data are stored in regular grids, the gradients can be approximated at any point using the two surrounding height values in each direction and the cellsize, as described by Rosenholm and Torlegård (1988) and Pilgrim (1991). Using irregular data makes the gradient computation more complicated.

Third, the use of interpolation is one of the major issues associated with this surface matching method. Interpolation can be used with varying levels of complexity—from relatively simple bilinear methods using surrounding grid posts (Ebner and Strunz, 1988) to polynomial or least-squares fitting and kriging based on a larger surface patch (McCullagh, 1990). In this approach, a relatively simple plane-fitting interpolation has been used, based on the vertices of the enclosing triangle. Given the large number of points available in most surface modeling applications, the redundancy present is large, allowing poor approximations to be classified as outliers and be removed from the solution.

Fourth, the precision of the solution depends on the nature of the coefficients in Equation 1 as obtained by linearization of the surface matching observation equations. Of particular interest is the determination that the solution relies heavily on the surface gradients in the $X$ and the $Y$ axes. The existence of points within the DEM with surface slopes in opposing planes is imperative for determining all seven parameters, because without this condition the two surfaces will be unconstrained (Rosenholm and Torlegård, 1988; Habib *et al.*, 2001). Two flat surfaces being matched will allow only three parameters, $\omega$, $\phi$,

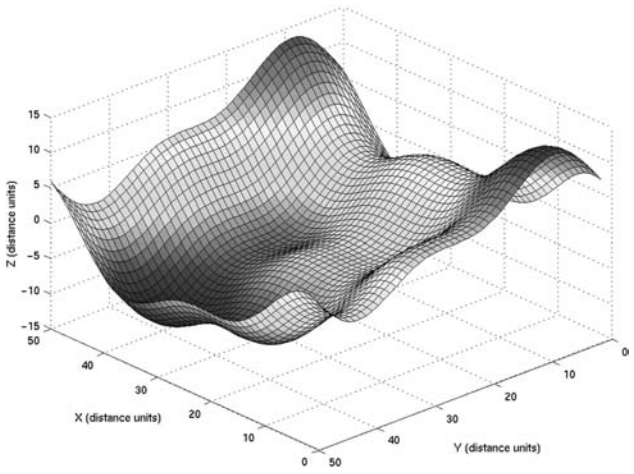


Figure 1. Simulated surface, Base, used in initial matching experiments.

and $T_z$, to be found, the lack of gradients in different directions giving unrealistic translation errors as the surfaces are free to slide across each other.

For these reasons, it can be expected that, if the two datasets are distinctly different or are sparse, the need to triangulate, interpolate, and extract gradients can make the efficacy of the matching difficult to predict.

## Testing the Surface Matching Algorithm

To determine the success of the surface matching algorithm, three levels of testing were carried out, with increasing degrees of complexity. Initial tests used simple simulated datasets to explore the capabilities and limitations of the surface matching program. The second stage of tests used photogrammetric and GPS-derived data to assess the capabilities of the algorithm when used with irregular datasets, raising a number of important issues. Finally, surfaces derived from small format aerial imagery and GPS were used, introducing more complex and dissimilar datasets in the real world coastal environment application.

### Matching of Simulated Surfaces

Prior to the use of any collected datasets, it was necessary to establish the validity of the matching algorithm, in terms of both theoretical and numerical outcomes. To achieve this, a series of five simulated surfaces were created using sine waves along the $X$ and $Y$ axes (Figure 1). One surface (Base) was used as control and the remaining surfaces (Test1 to Test4) were matched to Base. These simple surfaces comprised 50 by 50 grid points, and were identical except that the Test surfaces had mathematical transformations induced, as shown in Table 1. Using initial parameters of zero for rotations and translations, and one for scale, the shifts were expected to be the exact integer values induced in each direction with scale remaining uniform. Results from the simulated surface matches can be seen in Table 2. As further verification, and in order to remove the possibility of coding errors, these results were confirmed using two independently written matching programs.

From scrutiny of Table 2, it is apparent that the algorithm solved for the correct parameters, though with some errors, because the values were not exactly equal to the integer values originally used to transform the surfaces, except when Test1 was used as the second surface. Because the two surfaces were generated artificially, differences in data collection methods can be ignored. The remaining error was therefore due to the interpolation involved when the surfaces were out of alignment—when a true conjugate point existed and was matched, the result was zero units of translation being found, because the two points were already in the same system. Only when irregular or transformed data were used were errors introduced, because interpolation became necessary. Base/Test1 exemplifies this—the solution is correct because no interpolation was needed on the final iteration. In addition to interpolation error, differences between the surfaces being matched resulted in further errors in the final parameters (Karras and Petsa, 1993). Like interpolation, outlier and deformation detection is also a complex subject, with several studies having been carried out (Pilgrim, 1996; Li *et al.*, 2001). However, by analyzing the least-squares matrix of surface differences after each iteration, it is possible to reject points if the difference is greater than a specified tolerance. It should be noted now that although "errors" in the parameters are being classified, the match result might nevertheless be correct, because an equivalent but very slightly different set of parameters is found. The interpolation error in effect causes small artificial "deformations" between the surfaces, resulting in slightly different parameters.

Due to linearization of the surface matching observation equations, close initial parameter estimates were necessary for a solution to be found. The above tests on simulated surfaces were conducted using initial parameters of zero, so that only small transformation values were solved for. Further tests were carried out using increasingly incorrect initial parameters, with very similar solutions being obtained from up to 40° of rotation and 20 distance units of translation. The inclusion of the scale parameter, however, caused the solution to become unstable when estimates were poor. The nature of the test surfaces became an issue when these large parameter estimates were used, because the surface shape was not conducive to such values. Because the surfaces were generated artificially, based on sine waves in the $X$ and $Y$ axes, repetition of shape was found as the waves were repeated, having the effect that multiple solutions could be found. The user must be wary of such outcomes; because a match is found, the parameter standard deviations may be low, but the result incorrect.

Assuming a solution has converged and desired parameters have been found, it is then necessary to ascertain the validity of the match. Statistical information is useful but should not be wholly relied on, because any repetition in the surface shape may result in an alternate, but correct, match being

TABLE 1. TRANSFORMATIONS APPLIED TO SIMULATED SURFACES

| Parameter | Test1 | Test2 | Test3 | Test4 |
|---|---|---|---|---|
| Translation ($T_x$, $T_y$, $T_z$) (distance units) | 2.000 | 1.500 | 2.000 | 2.000 |
| | 2.000 | 1.500 | 2.000 | 2.000 |
| | 2.000 | 1.500 | 2.000 | 2.000 |
| Scale ($s$) | 1.000000 | 1.000000 | 1.000000 | 1.000000 |
| Rotation ($\omega$, $\phi$, $\kappa$)° | 0.000000 | 0.000000 | 2.000000 | 2.000000 |
| | 0.000000 | 0.000000 | 2.000000 | 2.000000 |
| | 0.000000 | 0.000000 | 2.000000 | 0.000000 |

TABLE 2. RESULTANT PARAMETERS AND RMS HEIGHT ERRORS FOR BASE AND TEST SIMULATED DATA. NOTE THAT PARAMETERS ARE NEGATIVE, BECAUSE THEY ARE THE AMOUNTS REQUIRED TO TRANSFORM THE TEST SURFACE INTO BASE

| Match result | Base/Test1 | Base/Test2 | Base/Test3 | Base/Test4 |
|---|---|---|---|---|
| Translation ($T_x$, $T_y$, $T_z$) (distance units) | −2.000 | −1.488 | −1.987 | −1.935 |
| | ±0.000 | ±0.001 | ±0.001 | ±0.002 |
| | −2.000 | −1.474 | −1.972 | −2.054 |
| | ±0.000 | ±0.002 | ±0.002 | ±0.002 |
| | −2.000 | −1.528 | −2.035 | −2.027 |
| | ±0.000 | ±0.001 | ±0.001 | ±0.002 |
| Scale ($s$) | 1.000000 | 0.999481 | 0.999601 | 0.999997 |
| | ±0.000000 | ±0.000033 | ±0.000031 | ±0.000043 |
| Rotation ($\omega$, $\phi$, $\kappa$)° | 0.000000 | 0.027049 | −1.973842 | −1.976038 |
| | ±0.000000 | ±0.002110 | ±0.001988 | ±0.002710 |
| | 0.000000 | −0.029251 | −2.031800 | −2.036678 |
| | ±0.000000 | ±0.001847 | ±0.001763 | ±0.002469 |
| | 0.000000 | −0.001241 | −2.008581 | 0.005618 |
| | ±0.000000 | ±0.001713 | ±0.001652 | ±0.002263 |
| RMS height error (distance units) | 0.000 | 0.017 | 0.016 | 0.023 |

found. Therefore, parameter standard deviations, residual statistics, and variance-covariance matrices only give an indication of match precision, not whether the result is "correct." Perhaps the most obvious way of verifying a match is by performing the transformation of the second surface using the final parameters and then carrying out a visual inspection of the two integrated surfaces. This immediately shows whether the two surfaces are in the correct system, because large surface errors will be visible. Additionally, examination of the least-squares residual matrix gives the errors between the surfaces, which will be small in a good match. Areas of large residuals may represent change or deformation occurring between data captured at different epochs.

#### Integration of an Analytical Photogrammetric DEM and GPS DEM

Before testing the matching algorithm on the complex coastal zone surfaces, a further test was carried out in a more controlled environment, using orthodox data collection techniques. A stereopair of the Town Moor, close to the city of Newcastle upon Tyne, UK, was chosen (Figure 2). This photography was captured in 1998 using a Leica RC10 large format camera at a flying height of 4000 feet (1200 m) with a focal length of 152 mm, giving a photoscale of approximately 1:8000. This photographic configuration provided a base/height ratio of 0.6 and a theoretical heighting precision of 0.03 m when measured in a first order analytical plotting instrument. A 250- by 250-m segment of this photography, containing a 30-m high grass mound, was deemed to be an ideal test site for creation of digital surfaces, due to the uninterrupted ground surface.

To follow the conventional photogrammetric processing chain, six GCPs were identified in the imagery and surveyed using static GPS procedures; these were then used to control the stereomodel in a Zeiss P3 analytical plotter. A DEM of the mound, with a grid spacing of 2.5 m, was manually measured using the semi-automated capture routine, creating a surface of 9278 points. The control surface used in this test was derived from GPS measurements. A wireframe model was created by following the rough shape of the hill, using the GPSycle (Buckley and Mills, 2001)—a standard surveyor's detail pole with a mountain bike wheel attached—and on-the-fly kinematic phase processing. Multiple height repeatability experiments using this methodology resulted in a standard deviation of 0.014 m along a known baseline, better than the expected pre-

Figure 2. 1:8,000-scale stereopair of Town Moor, Newcastle upon Tyne, UK. 250- by 250-m test area is boxed.

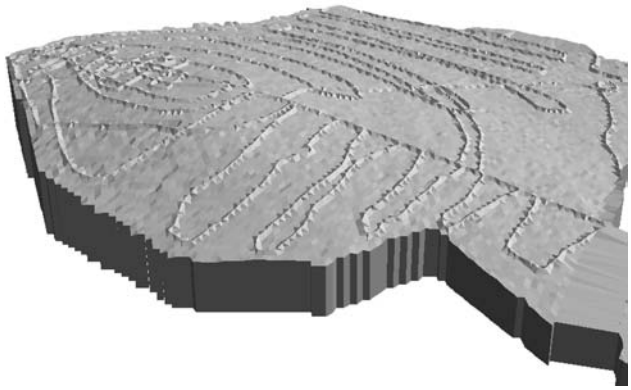

Figure 3. Unmatched Town Moor data, showing systematic difference between the photogrammetric and GPS surfaces. Approximate area of DEM is 250 by 250 m.

cision of the photogrammetry. Consequently, this sparse but highly accurate model was available as an alternative form of control using the matching program.

Because the photogrammetric DEM had been orientated using conventional ground control, it was expected that the post-match parameters would be close to zero, because the two surfaces were in the same reference system. Accordingly, initial parameters of zero were chosen for the rotations and translations and one for the scale factor; thus, any transformations found would be classified as errors either in data collection or in the matching. However, the length of the grass on the mound would have the consequence of introducing a small shift in the *Z* direction, because the GPS measured to the ground level and the photogrammetric DEM was measured to the top of the vegetation. This hypothesis was tested by carrying out a level difference check between the surfaces, resulting in an initial RMS error of 1.16 m. Closer examination revealed that the error was actually in the wrong direction, i.e., the photogrammetric surface was found to be *below* the GPS surface, as shown in Figure 3. This was confirmed when the matching was performed (Table 3).

Because of the greater disparities brought about by the different data collection methods, the solutions were slower to converge than when using the simulated data. As can be seen from Table 3, low rotation and translation values were obtained, including the larger *Z* translation required to merge the two surfaces. Varying the outlier removal tolerance or assuming uniform scale resulted in slightly different solutions being found; the parameter discrepancies between matches were therefore a result of the different points used in the solution, causing alternate "best-fit" positions to be found. The slightly larger than expected translation values were reflected in the parameter standard deviations, and here the effect of interpolation errors entering the solution can be seen, in a more pronounced way than with the simulated surface data.

Because the simulated data were stored in regular grids, triangulation of the surfaces resulted in equilateral triangles being formed, the ideal shape for interpolation to take place, due to the equal distances between vertices. However, because the GPS surface was comprised of lines of closely spaced points where data had been captured every second, it was very accurate in profile but when triangulated resulted in long thin triangles being formed (Figure 4). Because of this, when elevation and gradient values were interpolated at a point on the photogrammetric surface, the long distances between triangle vertices may have resulted in poor estimates.

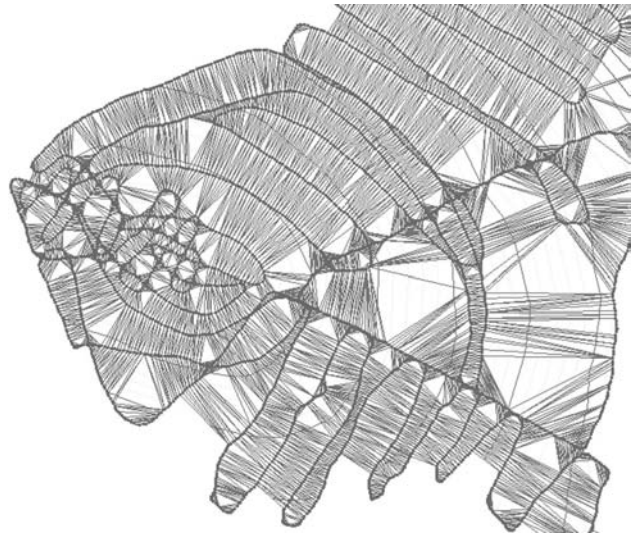

Figure 4. Delaunay triangulation of Town Moor GPS surface with 1-m contours.

TABLE 3. RESULTS OF MATCHES BETWEEN GPS AND PG (PHOTOGRAMMETRY) TOWN MOOR SURFACES. MATCHES WITH NO SCALE PARAMETER ASSUME UNIFORM SCALE

| Match result | GPS/PG | GPS/PG | GPS/PG | PG/GPS | PG/GPS |
|---|---|---|---|---|---|
| Exclusion tolerance (m) | none | 1.000 | 1.500 | none | 1.000 |
| Translation ($T_x$, $T_y$, $T_z$) m | 0.489 | 0.433 | 0.899 | −0.385 | −0.387 |
| | ±0.190 | ±0.184 | ±0.164 | ±0.076 | ±0.074 |
| | 1.329 | 1.247 | 1.139 | −0.594 | −0.977 |
| | ±0.214 | ±0.207 | ±0.081 | ±0.081 | ±0.036 |
| | 1.270 | 1.275 | 1.197 | −1.347 | −1.371 |
| | ±0.034 | ±0.033 | ±0.026 | ±0.019 | ±0.016 |
| Scale ($s$) | 0.998536 | 0.998906 | ~ | 0.998268 | ~ |
| | ±0.000769 | ±0.000742 | | ±0.000304 | |
| Rotation ($\omega$, $\phi$, $\kappa$)° | 0.006147 | 0.003202 | 0.016264 | 0.034342 | 0.034180 |
| | ±0.005484 | ±0.005306 | ±0.005041 | ±0.003626 | ±0.003526 |
| | −0.096347 | −0.100542 | −0.099601 | 0.085818 | 0.073809 |
| | ±0.005234 | ±0.005062 | ±0.003942 | ±0.003216 | ±0.002903 |
| | 0.223266 | 0.201593 | 0.295274 | −0.104020 | −0.121536 |
| | ±0.044691 | ±0.043227 | ±0.036622 | ±0.016265 | ±0.016231 |
| RMS height error (m) | 0.250 | 0.242 | 0.238 | 0.168 | 0.168 |

The effect of this interpolation error can be seen in the comparisons of the RMS errors and parameter standard deviations of the forward and reverse matches. Matching using the GPS surface as control produced an RMS error of 0.250 m, while using the photogrammetry surface as control resulted in a lower RMS error of 0.169 m, a trend that occurred for all matches with this dataset. This is assumed to occur because the regular grid structure of the photogrammetric DEM permits better interpolations of this form of data when matching the GPS surface to the photogrammetric DEM.

Like the simulated data, large amounts of error in initial parameters could be removed, again up to around 40° rotation and 50-m translation for all axes. However, altering the initial estimates resulted in slightly different parameters being found—to a greater extent than when using the simulated surfaces. In addition, use of the scale parameter with high initial errors resulted in the least-squares solution being singular.

The large error in the *Z* direction between the two surfaces was eliminated by the matching technique. However, it is important to establish where this large error originated so that it can be explained, similar effects having been seen in other projects using the same set of photography. Because the GPS track was corroborated with a known baseline, it was suspected that the camera calibration data were in error; the photography was captured in 1998, with a camera calibration certificate dated 1996. In this two-year period it is possible that the focal length of the RC10 camera had changed, making any processing of the set of photography in error accordingly. To verify this theory, a patch of the Moor model was remeasured with different camera focal lengths entered into the orientation. From the resultant DEMs it was found that using a +1-mm focal length, the DEM was 7 m below that created with the unmodified focal length. Similarly, the DEM created using focal length of -1 mm was found to be 7 m above the original DEM, suggesting a small error in the order of 0.2 mm was present in the focal length value quoted by the calibration certificate. Surface matching would therefore be a useful technique to check for calibration errors in archived photography, using ground areas where no surface discrepancies are found between data collection methods.

#### Absolute Orientation of Small Format Digital Imagery Using a GPS DEM

With successful matches of simulated and real world surfaces, the algorithm was used to match DEMs to a wireframe GPS surface created using small-format digital imagery, in a manner similar to the previous experiment. The area chosen for the experiment was Filey Bay, an 8.6-km stretch of coastline on the northeast coast of England and the location of an ongoing investigation into the optimum methodology for monitoring coastal erosion. Fieldwork for this dataset was conducted in August 2001, using a Kodak DCS660 camera mounted on a microlight platform to acquire aerial photography. The Kodak DCS660 is one in a succession of high-resolution digital SLR cameras; earlier cameras in the series had been used previously for mapping (Fraser, 1994; Mills *et al.*, 1996; Mason *et al.*, 1997) and surface modeling (Chandler *et al.*, 2001; Mills *et al.*, 2001). At a flying height of 2000 feet (600 m), the camera was set at ISO200 and the exposure was 1/400s at $f/4$ (Figure 5). The camera lens was a 28-mm Nikkor, resulting in an approximate photoscale of 1:22,000. With 9-$\mu$m square elements in the CCD array, this configuration provided a ground pixel size of 0.2 m and, with a base/height ratio of 0.4, an expected heighting precision of 0.35 m (Light, 2001). Because of the small format of the camera, around 50 images were required to give complete stereo coverage of the Filey Bay strip; hence, collection of ground control would have been inefficient.

Four areas in the bay (identified as CPK, TOW, GLF, and HUN) were chosen as test sites for accuracy assessments. For each of these, control stations were established and profiles of the beach and cliff areas were measured using a Leica TCR307 total station. The total station data, with 7-arc second angle measurement precision and 2-mm + 2-ppm distance measurement precision, were collected for use in match verification. A GPS wireframe model was captured using Leica System 500 dual frequency receivers, using the method described previously, to give the control surface for each test area. Because of the high data capture rate needed for on-the-fly phase processing of GPS data, some surface thinning was needed, because the difficult terrain resulted in the occasional build up of points over a small area, creating multiple small surface patches in the Delaunay triangulation.

Imagery was processed in LH Systems' SOCET Set version 4.3.1 digital photogrammetric workstation. A characteristic of SOCET Set is that some form of ground control is required to perform orientation, because the software attempts to solve both relative and absolute orientations simultaneously, obviously a detrimental requirement for this research. To negate this, three GCPs were scaled from existing mapping and measured in one stereopair of imagery of the north end of the bay. Utilizing the aerial triangulation capabilities of SOCET Set, further images were then added, each orientated with tie points, to give a continuous strip of imagery. Because of the poor distribution and accuracy of the ground control, the transformation grew increasingly inaccurate towards the end of the strip, with the

Figure 5. 1:22,000-scale near-vertical image (left) and oblique image (right) of CPK test area, captured using Kodak DCS660 camera. Boxed test area is approximately 180 by 200 m.

photogrammetric DEM being rotated slightly, and approximately 60 m below the GPS surface. Therefore, surface matching was crucial to provide orientation to the photogrammetric models.

Elevation models with a 2-m grid resolution were extracted automatically in SOCET Set for each of the four test areas. These were then matched to the corresponding GPS control surfaces, with results shown in Table 4. The four test areas were chosen so that they were well distributed along the strip: site CPK and site TOW were situated where the three control points were measured, site GLF was in the middle of the strip, and HUN was at the end of the strip. It was expected that, because of the decreasing accuracy of the transformation along the strip, the magnitude of the parameters would increase as distance from the control increased. Table 4 shows that this was indeed the case, with much larger parameters needed to match the HUN surface, at the end of the strip, to the GPS control.

A major issue encountered when using the Filey Bay data was the level of difference between the photogrammetric and GPS surfaces, brought about by actual surface differences and different surface interpolations. For the Town Moor data, this had been less of a problem, because the smooth nature of the mound meant that the GPS and photogrammetry agreed very closely in terms of surface shape. However, because of the more complex disposition of the Filey Bay data, the GPS breaklines were only discrete representations of the true surface, having implications on interpolation where localized surface roughness was present. In addition, the increased levels of vegetation and surface objects created areas of true difference, due to the point of measurement of the two techniques being different. These surface discrepancies were reflected in the RMS errors of the matches, higher than the expected heighting precision of the image configuration (Light, 2001). Use of the outlier exclusion tolerance was found to be of greater influence for these data, with parameters changed according to the level of difference suppressed. Examination of the post-match residuals highlights areas of error, such as the top and toe of the cliff where the actual surface has different interpolations, as well as vehicles, vegetation, and occasional buildings, where the two data collection methods differ (Figure 6).

The match results were assessed using the total station profiles measured at each of the test areas. The photogrammetric DEMs were transformed into the object-space coordinate system using the post-match parameters and then were merged with the GPS surface, giving single fused elevation models (Figure 7). Sections of these were then taken and compared with the total station data for each of the control stations in the areas, by inspecting the differences and correlation values between the profiles. In all cases the merged GPS and photogrammetric DEMs

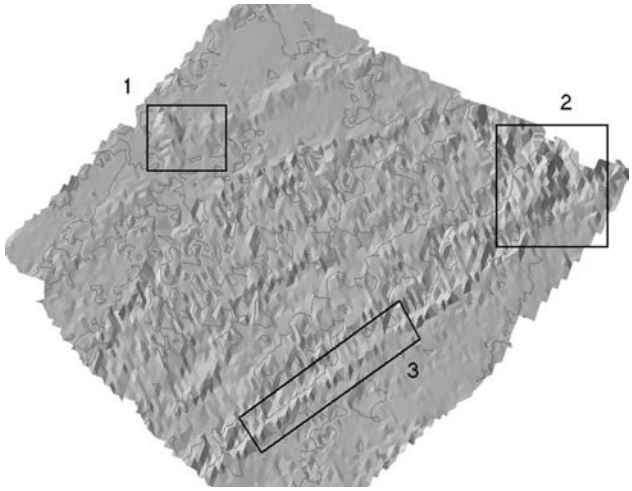


Figure 6. Residual plot of CPK test site, showing post-match differences between GPS and photogrammetric surfaces. Artefacts in the plot can be identified as vehicles (box 1) and areas where the two surfaces follow a different interpolation (box 2), such as the cliff toe (box 3). Zero-meter contour line plotted. Size of area is approximately 180 by 200 m.

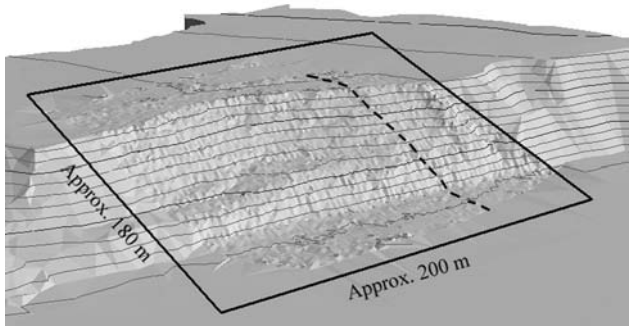


Figure 7. Merged CPK surface surrounded by wireframe GPS DEM alone (3-m contours). Total station profile line is dotted.

TABLE 4. MATCH RESULTS FOR FILEY BAY TEST AREAS

| Match result | GPS/CPK | GPS/TOW | GPS/GLF | GPS/HUN |
|---|---|---|---|---|
| Exclusion Tolerance (m) | 1.500 | 1.500 | 1.500 | 1.500 |
| Translation ($T_x$, $T_y$, $T_z$) m | 3.086 | 5.286 | −4.412 | 19.957 |
| | ±0.404 | ±0.365 | ±0.285 | ±0.430 |
| | 7.557 | 17.921 | −0.722 | 41.876 |
| | ±0.671 | ±0.718 | ±0.577 | ±0.578 |
| | −4.014 | 2.547 | −18.285 | 62.103 |
| | ±0.170 | ±0.156 | ±0.128 | ±0.207 |
| Scale ($s$) | 0.992222 | 0.975190 | 1.005417 | 0.982077 |
| | ±0.000593 | ±0.000892 | ±0.000885 | ±0.000846 |
| Rotation ($\omega$, $\phi$, $\kappa$)° | 0.255224 | 0.171311 | 0.626218 | 1.255421 |
| | ±0.009304 | ±0.012333 | ±0.09374 | ±0.013330 |
| | −0.040679 | 0.705590 | −0.541168 | −2.323968 |
| | ±0.010122 | ±0.013605 | ±0.016887 | ±0.014212 |
| | 0.008009 | 0.017138 | 0.030151 | 0.349077 |
| | ±0.023150 | ±0.026340 | ±0.024927 | ±0.025561 |
| RMS height error (m) | 0.452 | 0.477 | 0.564 | 0.486 |

TABLE 5. RMS ERRORS BETWEEN TOTAL STATION AND MERGED GPS AND PHOTOGRAMMETRIC PROFILES

| Profile | RMS (m) |
|---|---|
| CPK | 0.508 |
| TOW | 0.261 |
| GLF | 0.336 |
| HUN | 0.544 |

exhibited higher correlation with the total station data than using the GPS surface alone, up to 0.98. In addition, the differences between the profiles were of magnitudes similar to the matching RMS values (Table 5), with some deviation in the cliffs where the data followed a different interpolation of the "true" surface shape (Figure 8).

As further validation, the fused CPK DEM was compared with a set of pre-marked control targets, laid prior to the photographic mission. Fifty-four one-meter-diameter white circular discs had been laid within the model area and coordinated with the total station. Using these check points to determine the level difference with the merged CPK DEM resulted in an RMS error of 0.226 m, less than the matching RMS error, and better than the expected height precision of the photographic configuration. In addition, a further test was performed controlling the CPK model conventionally using six GCPs and extracting a DEM. Comparison of this DEM with the check points produced an RMS error of 0.749 m, suggesting that the expected measurement precision of the digital photography (0.35 m) was optimistic, and that the merged DEM had a better precision than the conventionally oriented DEM.

Continuity between adjacent DEMs, which are derived from the same photogrammetric strip orientation but which are matched separately to the control, is not yet assured. Because the surface matching solution finds the local best fit parameters for each photogrammetric DEM, any overlap between neighbouring surfaces should result in zero surface difference. However, as mentioned previously, any errors in the solution brought about by differences between the two surfaces will affect the final parameters, thus having the potential for error between overlapping points. Research on this aspect is ongoing.

## Conclusions

This paper has demonstrated the efficacy of surface matching to fuse DEMs derived from different data collection methods. In addition, the technique has the ability to recover systematic or transformation errors between measured and absolute control surfaces. Three individual sets of test data have been used, each developing the matching algorithm and addressing the issues associated with surfaces of increasing complexity. Use of simulated data, tested using two independently written matching programs, has confirmed theoretical aspects and the basic algorithm. A controlled experiment using conventional large-format metric aerial photography and a wireframe GPS elevation model has shown the application of surface matching to a real world dataset, highlighting the use of matching for irregular and dissimilar surfaces. Finally, the application of surface matching to strips of small-format digital imagery has proved successful in relating more complex terrain surfaces, thus removing the need for large amounts of photocontrol.

Although this paper has demonstrated the integration of photogrammetric and GPS elevation models, it can equally be applied to other aspects of geomatics where digital surfaces are involved. The surface matching algorithm is not dependent on the use of small-area topographic surfaces, but is also suitable for use with "national" level DEMs (Ebner and Strunz, 1988), as well as close-range and micro-scale applications (Karras and Petsa, 1993; Mitchell and Chadwick, 1999). For each application, the acquisition and scale of the control surface is important. For a DEM created from many large-format aerial images, it would be impractical to collect a wireframe GPS DEM. However, the existence of a coarse model available from many national mapping agencies would be applicable in this case. In a similar manner, surface matching may be employed to validate the integrity of laser scan data, by using existing control DEMs.

The surface matching algorithm has proved to be a flexible and effective technique for the integration of topographic surfaces, the high redundancy and potential for automation creating a useful substitute for photocontrol. However, like all digital procedures, care is needed in the use of surface matching: although a match may converge with high statistical evidence, the result may not be realistic, and as such the technique should not be treated as a "black box" technology.

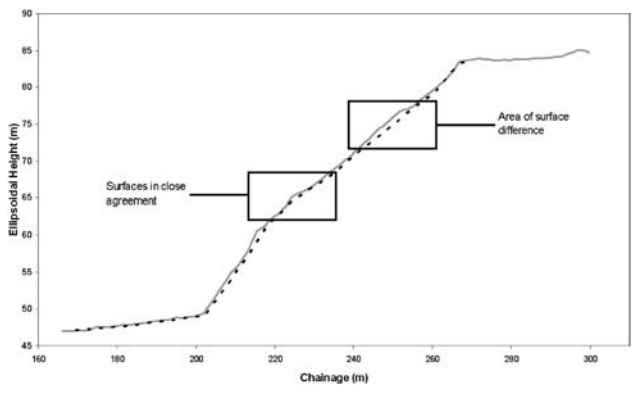


Figure 8. Example cliff profile comparison between merged GPS/photogrammetric DEM (solid line) and total station profile (dotted line) for CPK area.

## Acknowledgments

The authors appreciate the support of Scarborough Borough Council, Geotechnologies of Bath and Baxby Airsports Club, UK for fieldwork assistance. Thanks to David Loescher of LH Systems for assistance with photogrammetric processing. This research is funded by the Engineering and Physical Sciences Research Council (EPSRC), UK, grant GR/N23721.

## References

Adams, J.C., and J.H. Chandler, 2002. Evaluation of lidar and medium scale photogrammetry for detecting soft-cliff coastal change, *Photogrammetric Record*, 17(99):405–418.

Baltsavias, E.P., E. Favey, A. Bauder, H. Bösch, and M. Pateraki, 2001. Digital surface modelling by airborne laser scanning and digital photogrammetry for glacier monitoring, *Photogrammetric Record*, 17(98):243–274.

Besl, P.J., and N.D. McKay, 1992. A method for registration of 3D shapes, *IEEE Transactions on Pattern Analysis and Machine Intelligence*, 14(2):239–256.

Brunsden, D., and J.H. Chandler, 1996. Development of an episodic landform change model based upon the Black Ven mudslide, 1946–1995, *Advances in Hillslope Processes, Volume II* (M.G. Anderson and S.M. Brookes, editors), John Wiley and Sons, New York, N.Y., pp. 869–896.

Buckley, S., and J. Mills, 2001. Synergy of new geomatics technologies for coastal zone studies, *Engineering Surveying Showcase*, 2001(2):29–31.

Chandler, J.H., K. Shiono, P. Rameshwaren, and S.N. Lane, 2001. Measuring flume surfaces for hydraulics research using a Kodak DCS460, *Photogrammetric Record*, 17(97):39–62.

Cooper, M.A.R., 1998. Datums, coordinates and differences, *Landform Monitoring, Modelling and Analysis* (S.N. Lane, K.S. Richards, and J.H. Chandler, editors), John Wiley and Sons, New York, N.Y., pp. 21–35.

Cramer, M., D. Stallman, and N. Haala, 2000. Direct georeferencing using GPS/inertial exterior orientations for photogrammetric applications, *International Archives of Photogrammetry and Remote Sensing*, 33(B3):198–205.

Ebner, H., and G. Strunz, 1988. Combined point determination using digital terrain models as control information, *International Archives of Photogrammetry and Remote Sensing*, 27(B11): 578–587.

Fraser, C.S., 1994. Large scale mapping from small format imagery, *International Archives of Photogrammetry and Remote Sensing*, 30(4):332–337.

Habib, A., D. Kelley, and A. Asmamaw, 2000. New approach to solving matching problems in photogrammetry, *International Archives of Photogrammetry and Remote Sensing*, 33(B2):257–264.

Habib, A.F., Y.-R. Lee, and M. Morgan, 2001. Surface matching and change detection using a modified Hough transformation for robust parameter estimation, *Photogrammetric Record*, 17(98):303–315.

Karras, G.E., and E. Petsa, 1993. DEM matching and detection of deformation in close-range photogrammetry without control, *Photogrammetric Engineering & Remote Sensing*, 59(9):1419–1424.

Li, Z., Z. Xu, M. Cen, and X. Ding, 2001. Robust surface matching for automated detection of local deformation using least-median-of-squares estimation, *Photogrammetric Engineering & Remote Sensing*, 67(11):1283–1292

Light, D., 2001. An airborne direct digital imaging system, *Photogrammetric Engineering & Remote Sensing*, 67(11):1299–1305.

Maas, H.-G, 2000. Least-squares matching with airborne laserscanning data in a TIN structure, *International Archives of Photogrammetry and Remote Sensing*, 33(B3):548–555.

Mason, S., H. Ruther, and J. Smit, 1997. Investigation of the Kodak DCS460 digital camera for small-area mapping, *ISPRS Journal of Photogrammetry and Remote Sensing*, 52(5):202–214.

McCullagh, M.J., 1990. Digital terrain modelling and visualisation, *Terrain Modelling in Surveying and Civil Engineering* (G. Petrie and T.J.M. Kennie, editors), McGraw-Hill., Inc, New York, N.Y., pp. 128–151.

Mills, J.P., I. Newton, and R.W. Graham, 1996. Aerial photography for survey purposes with a high resolution, small format, digital camera, *Photogrammetric Record*, 15(88):575–587.

Mills, J.P., I. Newton, and G.C. Peirson, 2001. Pavement deformation monitoring in a rolling load facility, *Photogrammetric Record*, 17(97):7–24.

Mitchell, H.L., and R.G. Chadwick, 1999. Digital photogrammetric concepts applied to surface deformation studies, *Geomatica*, 53(4): 405–414.

Pilgrim, L.J., 1991. *Simultaneous Three Dimensional Object Matching and Surface Difference Detection in a Minimally Restrained Environment*, Research Report No. 066.08.1991, University of Newcastle, Newcastle, Australia, 172 p.

Rosenholm, D., and K. Torlegård, 1988. Three-dimensional absolute orientation of stereo models using digital elevation models, *Photogrammetric Engineering & Remote Sensing*, 54(10):1385–1389.

Schenk, T., 1999. *Digital Photogrammetry*, Terrascience, Laurelville, Ohio, 428 p.

Warner, W.S., R.W. Graham, and R.E. Read, 1996. *Small Format Aerial Photography*, Whittles Publishing, Caithness, Scotland, 348 p.

Wolf, P.R., and B.A. Dewitt, 2000. *Elements of Photogrammetry (with Applications in GIS), Third Edition*, McGraw-Hill, Inc., New York, N.Y., 624 p.

(Received 18 February 2002; accepted 10 April 2002; revised 20 June 2002)